J Appl Physiol 106: 1038–1049, 2009.
First published February 5, 2009; doi:10.1152/japplphysiol.90769.2008.

The effect of remifentanil on respiratory variability, evaluated with dynamic modeling

G. D. Mitsis,[1,2,3,4] R. J. M. Governo,[3,5] R. Rogers,[2,3] and K. T. S. Pattinson[2,3]

[1]*Institute of Communications and Computer Systems, National Technical University of Athens, Athens, Greece;* [2]*Nuffield Department of Anaesthetics, University of Oxford, Oxford, United Kingdom;* [3]*Oxford Centre for Functional Magnetic Resonance Imaging of the Brain, University of Oxford, Oxford, United Kingdom;* [4]*Department of Electrical and Computer Engineering, University of Cyprus, Nicosia, Cyprus, and* [5]*Brighton and Sussex Medical School, University of Sussex, Brighton, East Sussex, United Kingdom*

Submitted 15 June 2008; accepted in final form 2 February 2009

Mitsis GD, Governo RJ, Rogers R, Pattinson KT. The effect of remifentanil on respiratory variability, evaluated with dynamic modeling. *J Appl Physiol* 106: 1038–1049, 2009. First published February 5, 2009; doi:10.1152/japplphysiol.90769.2008.—Opioid drugs disrupt signaling in the brain stem respiratory network affecting respiratory rhythm. We evaluated the influence of a steady-state infusion of a model opioid, remifentanil, on respiratory variability during spontaneous respiration in a group of 11 healthy human volunteers. We used dynamic linear and nonlinear models to examine the effects of remifentanil on both directions of the ventilatory loop, i.e., on the influence of natural variations in end-tidal carbon dioxide ($P_{ET}CO_2$) on ventilatory variability, which was assessed by tidal volume (VT) and breath-to-breath ventilation (i.e., the ratio of tidal volume over total breath time VT/TTOT), and vice versa. Breath-by-breath recordings of expired CO_2 and respiration were made during a target-controlled infusion of remifentanil for 15 min at estimated effect site (i.e., brain tissue) concentrations of 0, 0.7, 1.1, and 1.5 ng/ml, respectively. Remifentanil caused a profound increase in the duration of expiration. The obtained models revealed a decrease in the strength of the dynamic effect of $P_{ET}CO_2$ variability on VT (the "controller" part of the ventilatory loop) and a more pronounced increase in the effect of VT variability on $P_{ET}CO_2$ (the "plant" part of the loop). Nonlinear models explained these dynamic interrelationships better than linear models. Our approach allows detailed investigation of drug effects in the resting state at the systems level using noninvasive and minimally perturbing experimental protocols, which can closely represent real-life clinical situations.

nonlinear models; Volterra kernels; opioid; ventilation; chemoreflex

RESPIRATORY DEPRESSION is the most common serious side effect of opioid drugs (32). Opioids are prescribed to millions of patients around the world every day, often in unmonitored environments, and therefore avoiding respiratory depression remains an important clinical aim. Opioids depress chemosensitive and rhythm-generating centers in the brain stem (13, 26), leading to slowing and irregularity of the respiratory rhythm (4, 22).

In rodents opioids cause interruption of the output from the rhythm-generating centers in the ventral lateral medulla of the brain stem [i.e., the pre-Bötzinger complex and the retrotrapezoid nucleus (26)], irregular respiration being caused by intermittent "skipped" outputs from the pre-Bötzinger complex. Three studies in humans (4, 14, 22) have demonstrated changes in respiratory timing with opioids, but none of these studies has explored potential mechanisms and how changes in timing may relate to changes in chemoreflex responsiveness.

Much of the understanding of human respiratory control is based on characterization of the ventilatory feedback loop, which is shown in Fig. 1 in a simplified form, supplemented by inferences from work in animals. The standard approach is to examine ventilatory responses to hypoxic or hypercapnic (31, 34) stimulation; specifically, depression of these responses by opioids has been well reported (2, 10, 11). Moreover, breath-to-breath fluctuations in end-tidal CO_2 ($P_{ET}CO_2$) are responsible for a considerable fraction of the normal variability in tidal volume (VT) during spontaneous breathing (29), and the dynamic effects of these spontaneous fluctuations have been used to derive information on ventilatory feedback (18, 36). This breath-to-breath variability has been modulated with background hyper- and hypocapnia (5, 15) but has not yet been applied to investigation of drug action.

Remifentanil is a short-acting opioid analgesic that is used in anesthesia. Its ultrashort context-insensitive half-life (3–4 min) allows rapid adjustment of plasma levels when infused using a computer-controlled pump preprogrammed with a pharmacokinetic model of the drug (target-controlled infusion) (27, 28). The short half-life means that it can be given by infusion and plasma levels can be changed rapidly. In terms of volunteer safety, it is possible to achieve a relatively strong opioid effect with remifentanil, but if there are any signs of adverse drug reaction, the infusion can be terminated with the confidence that the drug will wear off within minutes.

Here, we have examined the effect of remifentanil infusion on respiratory variability by quantifying the dynamic interrelationships between $P_{ET}CO_2$, VT, and breath-to-breath ventilation (i.e., VT/TTOT, where TTOT is total breath time) in both causal directions of the ventilatory loop. We examined the relationship between $P_{ET}CO_2$ and VT because we were interested in examining how motor output (VT) may be affected independently of respiratory rate. As ventilation (VT/TTOT) is a more conventional measure of respiration, we have also assessed this variable so that our results can be compared with other studies of respiratory control. To achieve this, we have used a nonlinear, data-driven modeling approach (Laguerre expansion technique) that has been used extensively in physiological systems modeling (24, 25). First, we considered the dynamic influence of spontaneous $P_{ET}CO_2$ fluctuations on ven-

Address for reprint requests and other correspondence: G. D. Mitsis, Dept. of Electrical and Computer Engineering, Univ. of Cyprus, PO Box 20537, Kallipoleos 75, Nicosia 1678, Cyprus (e-mail: gmitsis@ucy.ac.cy).

The costs of publication of this article were defrayed in part by the payment of page charges. The article must therefore be hereby marked "*advertisement*" in accordance with 18 U.S.C. Section 1734 solely to indicate this fact.

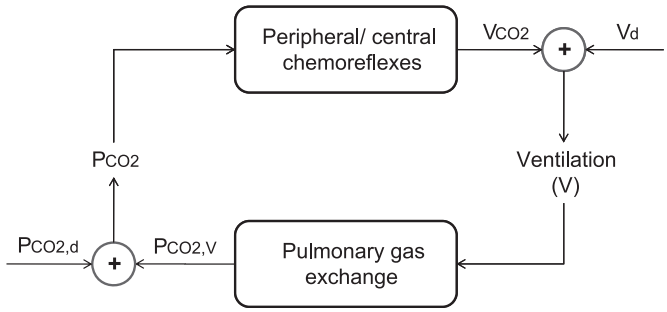

Fig. 1. Simplified block diagram of the ventilatory loop. Spontaneous ventilatory variability [assessed by tidal volume (V_T) and the ratio of tidal volume to total breath time (V_T/T_{TOT})] arises from a chemical component V_{CO2} that is due to variations in arterial CO_2 tension variability (P_{CO_2}), and a nonchemical component V_d (disturbance term, which includes sighs) that is due to all other physiological influences. Similarly, spontaneous P_{CO_2} variability arises from a ventilatory-related component $P_{CO_{2,V}}$ that is due to variations in V_T, and a nonventilatory related component $P_{CO_{2,d}}$.

tilatory variability (the forward part of the ventilatory loop), whereby the latter was assessed by V_T and breath-to-breath ventilation. Subsequently, we examined the influence of ventilatory variability on $P_{ET_{CO_2}}$ (the reverse part of the ventilatory loop) by reversing the roles of input and output. As respiratory control mechanisms are likely to exhibit nonlinear dynamics (15), we compared the performance of linear and nonlinear (Volterra) models in describing the dynamic interrelationships between $P_{ET_{CO_2}}$ and respiratory variability. We hypothesized that remifentanil, by depressing chemoreceptor responsiveness, would decrease the influence of $P_{ET_{CO_2}}$ fluctuations on ventilatory variability. On the other hand, we were unsure whether the relationship between ventilatory variability and $P_{ET_{CO_2}}$ variability would remain unaffected. The results illustrate the potential of applying systems identification/modeling techniques to the investigation of drug-induced changes on respiratory control. These techniques allow the extraction of useful information during spontaneous breathing, i.e., during conditions that mimic real-life clinical situations.

METHODS

Subjects

This study was approved by the Oxfordshire Clinical Ethics research committee, and volunteers gave written informed consent. Eleven healthy volunteers (3 women; mean age ± SD, 27 ± 5 yr) were examined, recruited by advertisement within Oxford University. Volunteers were excluded if they were taking medication or drugs acting on the central nervous or respiratory systems for therapeutic or recreational use. A medical history and, where appropriate, a physical examination were performed to ensure that the subjects were healthy (American Society of Anesthesiologists physical status 1) and that there was no contraindication to remifentanil. Volunteers fasted before all visits (6 h for solids, 2 h for clear fluids) and were supervised for 1 h following termination of the infusion.

Experimental Protocol

The subjects wore a tight-fitting facemask (Hans Rudolph), which was attached to a modified T-piece breathing system (23). The resistance to breathing was kept minimal by using wide-bore (diameter 8 cm) respiratory tubing, which also allows rapid alterations of inspired gas concentrations, when combined with high fresh gas flow rates (this breathing system is particularly useful during studies where there is high minute ventilation, for example during exercise). The fresh gas flow rate was 30 l/min to eliminate rebreathing of expired gases. Respiratory depression may cause hypoxemia, which causes activation of peripheral chemoreceptors in the carotid bodies and stimulates respiration. In this study, end-tidal oxygen ($P_{ET_{O_2}}$) tension was maintained at 30 kPa by manual adjustment of the inspired gas mixture by a dedicated experimenter, on a breath-by-breath basis, to maintain peripheral chemoreceptor input constant. The subjects were asked to keep their eyes open throughout and watched a movie to distract them from the experiment.

A target-controlled infusion of remifentanil (at a solution concentration of 10 μg/ml) was delivered via an indwelling intravenous cannula inserted into a vein in the left forearm. Stepwise ascending effect site concentrations (i.e., based on predicted brain concentrations) of zero (baseline), 0.7, 1.1, and 1.5 ng/ml were maintained with a computer-controlled infusion pump (Graseby 3500 TCI incorporating "Diprifusor", SIMS Graseby) (17) that was preprogrammed according to a pharmacokinetic model of remifentanil (27, 28). We chose to investigate remifentanil because effect site concentrations are easily manipulated due to its short context-insensitive half-life, and therefore we could maintain stable effect site concentrations during the experiment. We also chose relatively low doses of remifentanil so that we could investigate the subtle changes in respiratory control seen at clinically relevant opioid analgesia, as opposed to the much higher doses used in anesthesia. Our previous experimental experience with this drug found that subjects became apneic or fell asleep at effect site concentrations greater than 2 ng/ml in similar studies without painful stimuli.

Oxygen saturations, heart rate, $P_{ET_{CO_2}}$, and $P_{ET_{O_2}}$ were monitored continuously using a Datex Cardiocap II (Datex Instrumentarium, Helsinki, Finland), and respiratory volume and timing were measured with a turbine respiratory flowmeter (VMM-400, Interface Associates, Laguna Niguel, CA) and recorded with a data-acquisition device sampling at 50 Hz (PowerLab 8, ADInstruments, Colorado Springs, CO) connected to a laptop computer using dedicated software (Chart 5, ADInstruments).

As this experiment was designed to measure respiratory variability during spontaneous breathing, there was no specific experimental task for the subjects to perform. Following a minimum of 10 min to adapt to the mask, the baseline recordings (i.e., no remifentanil infusion) were taken for 15 min, and then for each level of remifentanil. Five minutes was allowed to reach target effect site concentration (as displayed on the infusion device); continuous recordings were made for the following 15 min at that stable effect site concentration.

Dynamic Modeling

After linear detrending to remove the effect of very slow trends, the dynamic effects of natural variations in $P_{ET_{CO_2}}$ on V_T and V_T/T_{TOT}, and vice versa, were quantified by using a variant of the Volterra-Wiener approach (24). In this context, we employed the general Volterra model, which is given below for a Qth-order nonlinear system:

$$y(n) = \sum_{q=0}^{Q} \sum_{m_1=0}^{M} \cdots \sum_{m_q=0}^{M} k_q(m_1, \ldots, m_q)x(n - m_1) \ldots x(n - m_q)$$
$$= k_0 + \sum_{m=0}^{M} k_1(m)x(n - m) + \sum_{m_1=0}^{M} \sum_{m_2=0}^{M} k_2(m_1, m_2)x(n - m_1)x(n - m_2) + \ldots \quad (1)$$

where $x(n)$ and $y(n)$ are the system input and output, respectively (as mentioned above, both $P_{ET_{CO_2}}$ and V_T or V_T/T_{TOT} assume the roles of input and output), M is the system memory, and $k_q(m_1, \ldots, m_q)$ are the Volterra kernels of the system, which describe the linear ($Q = 1$) and nonlinear ($Q > 1$) dynamic effects of the input on the output. *Equation 1* reduces to the convolution sum for linear systems ($Q = 1$),

with $k_1(m)$ corresponding to the impulse response of the system. This approach has been employed extensively for modeling physiological systems, since it is well suited to their complexity (24).

The impulse response or Volterra kernels can be estimated efficiently from the input-output data, by utilizing function expansions in terms of the orthonormal Laguerre basis (25):

$$k_q(m_1, \ldots, m_q) = \sum_{j_1=0}^{L} \ldots \sum_{j_q=j_{q-1}+1}^{L} c_{j_1 \ldots j_q} b_{j_1}(m_1) \ldots b_{j_q}(m_q) \quad (2)$$

where $c_{j1 \ldots jn}$ are the expansion coefficients, $b_j(m)$ is the jth-order Laguerre function, and $L + 1$ is the total number of functions that yields an adequate system representation. By combining *Eqs. 1* and *2* in matrix form:

$$\mathbf{y} = \mathbf{Vc} + \boldsymbol{\varepsilon} \quad (3)$$

where the nth row of $\mathbf{V}$ is given by $[1, v_1(n), \ldots, v_L(n), (v_1(n))^2, v_1(n)\cdot v_2(n), \ldots, v_1(n)\cdot v_L(n), (v_2(n))^2, v_2(n)\cdot v_3(n), \ldots, (v_L(n))^2]$ for a second-order system ($Q = 2$), $\mathbf{c}$ is the vector of expansion coefficients, $\boldsymbol{\varepsilon}$ is the observation errors vector, which in our case includes the disturbance terms, and

$$v_j(n) = \sum_m b_j(m)x(n - m) \quad (4)$$

denotes the convolution of the input with the jth order Laguerre function. The expansion coefficients are then obtained by the least-squares solution of *Eq. 3* (25):

$$\mathbf{c_{est}} = [\mathbf{V^T V}]^{-1}\mathbf{V^T y} \quad (5)$$

Model performance was assessed by the normalized mean-square error (NMSE) of the output prediction, which is defined as the mean-squared model residuals divided by the corresponding mean-squared output. The NMSE is also used to determine the number of Laguerre functions $L + 1$ and system order Q, by using a statistical criterion to assess the significance of the NMSE reduction achieved by more complex (i.e., larger L, Q) model structures. Specifically, the percentage NMSE reduction achieved for models of increased complexity was compared with the α-percentile value of a chi-square distribution with p degrees of freedom (where p is the increase of the number of free parameters for more complex levels) at a significance level α of 0.05 (35).

Note that, for the chemoreflex pathway ($P_{ET_{CO_2}} \rightarrow$ V, where V corresponds to either V_T or V_T/T_{TOT}) sighs, which were defined as breaths with values greater than 1.5 times the mean breath value, were removed by linear interpolation before model estimation, following the approach described in Ref. 36. The reason is that sighs are not caused by $P_{ET_{CO_2}}$ changes; therefore, they are viewed as part of the disturbance (non-CO_2 dependent) component of V, denoted by V_d in Fig. 1. Note also that a pure time delay of two breaths was hypothesized in the effects of $P_{ET_{CO_2}}$, i.e., the V_T and V_T/T_{TOT} time series were shifted accordingly before model estimation, to account for the previously described transport delays in the action of $P_{ET_{CO_2}}$ (20, 34). On the other hand, sighs were not removed for the reverse pathway ($V \rightarrow P_{ET_{CO_2}}$), since they are a significant determinant of $P_{ET_{CO_2}}$ changes.

The linear and nonlinear components of the model of *Eq. 1, i.e.,* k_1 and k_2, respectively, were averaged over all subjects. Their characteristics in the frequency domain were obtained by computing their one-dimensional (k_1) and two-dimensional (k_2) discrete Fourier transform (DFT). The spectral power of the kernels was calculated by integrating these frequency domain characteristics from 0 to 0.3 cycles/breath in the case of k_1 and from [0 0] to [0.3 0.3] cycles per breath in the case of k_2.

Statistical Analysis

Changes in the steady-state values and the spectral power of the respiratory variables, which was calculated by integrating their power spectral density function (PSD; obtained using the Welch modified periodogram method), as well as in the spectral power of the first- and second-order kernels were assessed by using repeated-measures ANOVA, with P values of <0.05 considered significant (SPSS 16.0 for Windows, SPSS, Chicago, IL).

RESULTS

In no subject was there loss of consciousness, and all volunteers remained awake, with eyes open, and maintained verbal contact at all times. On no occasion did oxygen saturations fall below 96%. In one subject the infusion was terminated at an effect site concentration of 1.5 ng/ml due to persistent nausea.

Respiratory Variables

Steady-state values. The measured physiological variables are presented in Table 1. We observed a dose-dependent decrease in respiratory rate that was due to increases in dura-

Table 1. *Steady-state respiratory parameters*

		Remifentanil		
	Baseline	0.7 ng/ml	1.1 ng/ml	1.5 ng/ml
$P_{ET_{CO_2}}$, kPa	5.4 (0.3)	5.8 (0.4)†	5.9 (0.4)†	6.2 (0.6)†
CV $P_{ET_{CO_2}}$, %	2.4 (1.0)	3.7 (1.2)†	4.2 (2.7)†	4.3 (2.0)†
SP $P_{ET_{CO_2}}$	1.2 (1.1)	2.6 (1.5)†	3.3 (2.9)	4.0 (2.6)†
$P_{ET_{O_2}}$, kPa	30 (1)	30 (1)	30 (2)	29 (2)
V_T, ml	412 (134)	348 (128)*	360 (114)	384 (144)
CV V_T, %	40 (14)	49 (15)	59 (20)*	52 (10)*
SP V_T	$1.7\cdot10^5$ ($1.3\cdot10^5$)	$1.8\cdot10^5$ ($1.7\cdot10^5$)	$3.2\cdot10^5$ ($3.3\cdot10^5$)	$2.5\cdot10^5$ ($2.3\cdot10^5$)
T_I, s	1.5 (0.3)	1.6 (0.4)	1.6 (0.5)	1.6 (0.5)
CV T_I, %	25 (9)	25 (5)	28 (9)	29 (7)†
T_E, s	2.7 (0.4)	3.8 (0.8)†	4.7 (1.6)†	5.2 (2.1)†
CV T_E, %	21 (5)	26 (9)*	30 (8)*	39 (13)†
V_T/T_{TOT}, ml/s	100.2 (23.3)	64.0 (23.6)†	60.8 (20.6)†	61.5 (22.3)†
CV V_T/T_{TOT}, %	26.0 (8.2)	39.6 (6.8)†	48.5 (14.2)†	56.4 (22.0)†
SP V_T/T_{TOT}	436.0 (233.9)	494.2 (323.7)	658.9 (430.2)	989.4 (1,274.5)
HR, beats/min	56.8 (7.8)	55.8 (7.1)	54.8 (9.3)	55.9 (8.3)

Values are mean (SD). $P_{ET_{CO_2}}$, end-tidal CO_2; $P_{ET_{O_2}}$, end-tidal O_2; V_T, tidal volume per breath; T_E, expiratory time; T_I, inspiratory time; T_{TOT}, total breath time; HR, heart rate; CV, coefficient of variability; SP, spectral power between 0 and 0.3 cycles/ breath. *$P < 0.05$, †$P < 0.01$ with respect to baseline.

tion of expiratory time (T_E). We did not observe any change in inspiratory time (T_I). The variability coefficients of T_I and T_E increased, with a much stronger effect being observed for T_E. V_T initially decreased (at 0.7 ng/ml) but increased at higher levels toward baseline values. As a result, breath-to-breath ventilation V_T/T_{TOT} decreased and became progressively more variable. P_{ETCO_2} increased and became more variable. Finally, heart rate remained approximately constant.

Spectral power. The spectral power of P_{ETCO_2} and V_T was calculated by integrating their power spectral density (PSD) functions (Fig. 2). The upper limit of the integration was set to 0.3 cycles/breath, since the spectral power of both variables, as well as of the system dynamics examined below, was concentrated below this frequency. An increase over the entire frequency range (i.e., between 0 and 0.3 cycles/breath), which was gradual except below 0.02 cycles/breath (whereby the largest changes occurred for 0.7 ng/ml), was observed for the P_{ETCO_2} spectral power compared with baseline. V_T spectral power also increased during remifentanil infusion, but these changes were less pronounced and occurred above 0.02 cycles/breath.

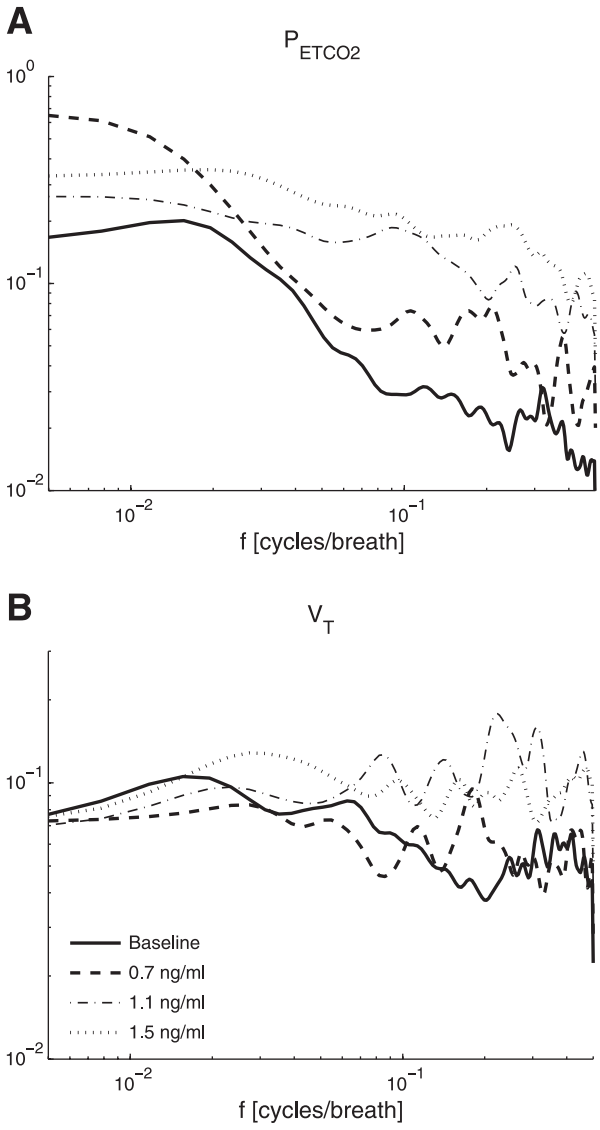

Fig. 2. Power spectral density function of the end-tidal carbon dioxide (P_{ETCO_2}) (*A*) and V_T (*B*) time series between 0 and 0.3 cycles/breath, averaged over all subjects (means ± SE). Note the gradual increase in the P_{ETCO_2} power induced by remifentanil over the entire frequency (f) range and the less pronounced increase in V_T spectral power above 0.02 cycles/breath.

Dynamic Modeling

Model performance. By following the procedure outlined in METHODS, it was found that five Laguerre functions ($L + 1 = 5$) are adequate to represent the system dynamics in both pathways. The prediction NMSEs obtained by linear and nonlinear models ($Q = 1,2$) for both pathways of the ventilatory loop, which correspond to the dynamic effects of P_{ETCO_2} variations on V_T or V_T/T_{TOT}, and vice versa, are given in Table 2. Nonlinear models improved model performance in both pathways, i.e., they resulted in significantly reduced prediction NMSEs, which satisfied the statistical criterion described in METHODS. For the forward part of the loop ($P_{ETCO_2} \rightarrow V$) we also observed a dose-dependent reduction in the NMSE values during remifentanil infusion in the case of nonlinear models, which suggests that a larger fraction of the respiratory variability is caused by P_{ETCO_2} changes. For the reverse branch of the ventilatory loop ($V \rightarrow P_{ETCO_2}$), remifentanil did not affect the NMSE values as above (Table 2).

Representative data sets used for model estimation (obtained during baseline) are shown in Fig. 3, along with the corresponding nonlinear model predictions in the time (Fig. 3, *left*) and frequency (PSD; Fig. 3, *right*) domain. To illustrate the contribution of the nonlinear model terms in the frequency domain, we also show the time trace and PSD of the corresponding linear model prediction (Fig. 3, *left*) and residuals (Fig. 3, *right*), respectively. Note that the sighs that are evident in the V_T time series (Fig, 3*B, left*, dotted line) are not explained by the $P_{ETCO_2} \rightarrow V_T$ model, as they were removed before estimation. P_{ETCO_2} variations mainly account for the V_T postsigh response, as sighs are clearly correlated with sharp P_{ETCO_2} drops (as expected), which in turn influence V_T. On the other hand, these sharp drops are evidently accounted by the $V_T \rightarrow P_{ETCO_2}$ model. In the frequency domain, the incorporation of nonlinear model terms improved performance over a wide range of frequencies below 0.03 Hz, particularly for the $V_T \rightarrow P_{ETCO_2}$ pathway (Fig. 3*A, right*). The aforementioned model residual characteristics were maintained when V_T/T_{TOT} was used to assess ventilatory variability. Overall, a larger fraction of P_{ETCO_2} variations was explained by the $V \rightarrow P_{ETCO_2}$ models compared with the reverse pathway, which is reflected on the lower NMSE values achieved by the $V \rightarrow P_{ETCO_2}$ models (Table 2; note again that sighs were not taken into account when calculating the $P_{ETCO_2} \rightarrow V$ NMSEs). The lower $P_{ETCO_2} \rightarrow V$ NMSE values during remifentanil infusion were mainly due to the more pronounced (compared with V_T, V_T/T_{TOT}) increased P_{ETCO_2} variability that was induced (Fig. 2).

System dynamics: $P_{ETCO_2} \rightarrow V$ pathway. The first-order kernel (k_1 in *Eq. 1*) corresponds to the impulse response of the system when linear models are used ($Q = 1$ in *Eq. 1*) and to the linear component of the system dynamics in the case of nonlinear models ($Q > 1$ in *Eq. 1*). The averaged impulse responses (i.e., obtained from linear models) for the forward part of the ventilatory loop are displayed in Fig. 4, when both V_T (blue) and V_T/T_{TOT} (black) were used to assess ventilatory

Table 2. *Prediction NMSEs for linear and nonlinear dynamic models for the forward and reverse pathways of the ventilatory loop*

	NMSE, %			
	Forward		Reverse	
	Linear	Nonlinear	Linear	Nonlinear
	$P_{ET_{CO_2}} \rightarrow V_T$		$V_T \rightarrow P_{ET_{CO_2}}$	
Baseline	87.6 (2.0)	71.0 (2.9)	71.1 (5.0)	53.3 (4.6)
Remifentanil				
0.7 ng/ml	87.3 (3.0)	62.6 (3.6)	67.5 (5.5)	46.6 (4.6)
1.1 ng/ml	89.4 (1.6)	62.1 (3.9)	79.7 (1.6)	58.8 (3.8)
1.5 ng/ml	87.1 (2.5)	57.9 (3.7)	78.6 (4.4)	54.3 (4.5)
	$P_{ET_{CO_2}} \rightarrow V_T/T_{TOT}$		$V_T/T_{TOT} \rightarrow P_{ET_{CO_2}}$	
Baseline	86.7 (1.7)	65.7 (2.8)	67.5 (4.4)	45.7 (4.8)
Remifentanil				
0.7 ng/ml	80.4 (5.1)	55.9 (4.3)	62.1 (8.1)	41.5 (5.5)
1.1 ng/ml	87.5 (1.3)	58.3 (3.9)	76.5 (3.2)	56.5 (3.7)
1.5 ng/ml	87.5 (1.2)	55.3 (4.6)	74.8 (4.7)	50.3 (4.8)

Nonlinear models reduce the normalized mean-square error (NMSE) significantly in all cases. See Fig. 1 for forward and reverse pathways of ventilatory loop.

variability. The form of the averaged impulse response during baseline suggests that an increase in $P_{ET_{CO_2}}$ will cause an increase in V_T (or V_T/T_{TOT}), with the maximum instantaneous effects occurring (on the average) at four and eight breaths after the $P_{ET_{CO_2}}$ increase (after taking into account the 2-breath pure time delay). The impulse response values generally decreased during remifentanil infusion, with the decrease being more evident for the second peak. An undershoot at 13 breaths was observed during baseline only, while a secondary positive peak between 15 and 20 breaths was also observed. Note that both measures of ventilatory variability yielded similar system dynamics, especially during baseline (Fig. 4, *top left*).

The impulse responses are shown in Fig. 5 in the frequency domain, averaged over all subjects. The characteristics of the impulse response in the frequency domain during baseline were consistent across subjects, with a main resonant peak occurring between 0.04 and 0.08 cycles/breath in 9 of the 11 subjects (and more specifically between 0.07 and 0.08 cycles/breath in 6 of 11 subjects). This suggests that $P_{ET_{CO_2}}$ oscillations at the corresponding cycles (i.e., between 12.5 and 25 breaths) will have a more pronounced effect on V_T (and V_T/T_{TOT}). As a result, a resonant peak at 0.07 cycles/breath was observed in the averaged frequency response. The impulse response spectral characteristics were less consistent during remifentanil infusion, with the main resonant frequency peak being shifted to lower frequencies in most cases. This is reflected in the averaged plots of Fig. 5, where the peak at 0.07 cycles/breath is not evident during remifentanil infusion. The frequency response of the second-order kernels (k_2 in *Eq. 1*), averaged over all subjects, is shown in Fig. 6 for V_T in the 2-dimensional frequency domain. The gain values

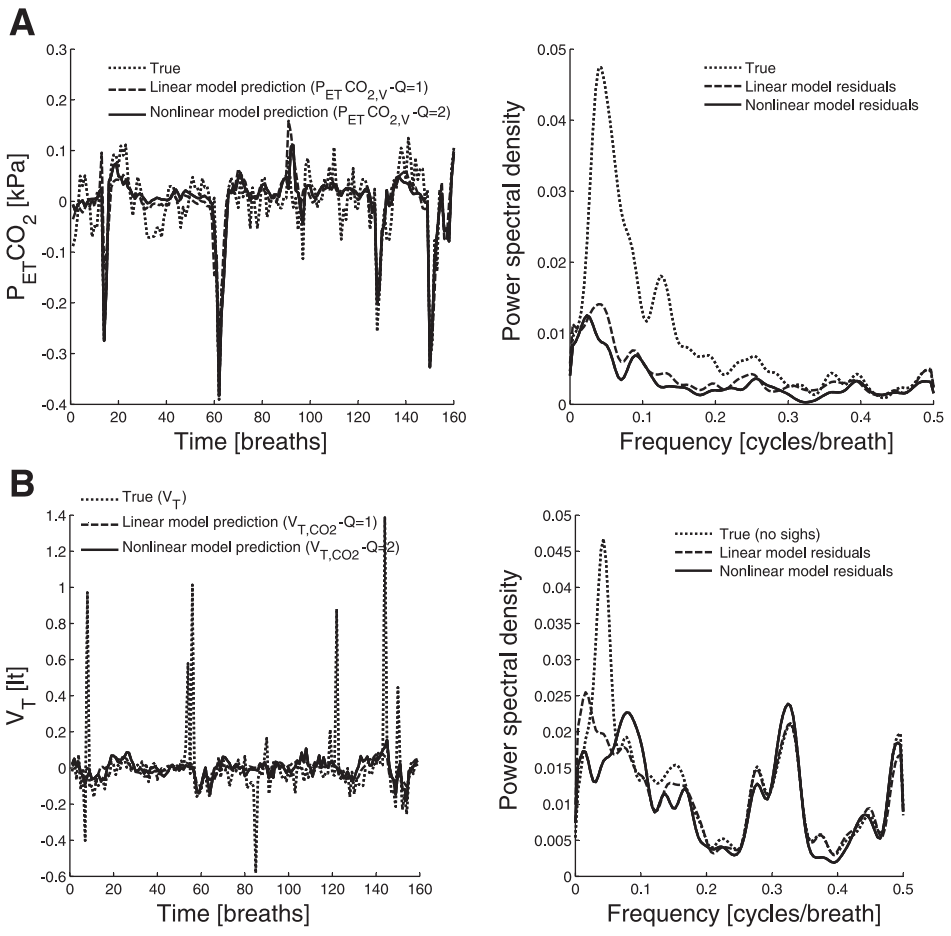

Fig. 3. *Left*: representative $P_{ET_{CO_2}}$ (*A*, *left*; dotted line) and V_T (*B*, *left*; dotted line) time series during baseline, used for model estimation in both pathways of the ventilatory loop, and corresponding nonlinear model predictions [$P_{ET_{CO_2,V}}$ (*A, left*) and V_{TCO2} (*B, left*), respectively; solid lines]. Note that the large drops in $P_{ET_{CO_2}}$ induced by deep breaths (sighs) are clearly accounted by the $V_T \rightarrow P_{ET_{CO_2}}$ model (*A*, *left*; solid line), while $P_{ET_{CO_2}}$ changes account mainly for the postsigh V_T response (*B*, *left*; solid line). *Right*: power spectral density of output signals (dotted lines), linear model residuals (dashed lines), and nonlinear model residuals (solid lines). The nonlinear model terms contributed over a wide range of frequencies, especially in the $V_T \rightarrow P_{ET_{CO_2}}$ pathway (*A, right*).

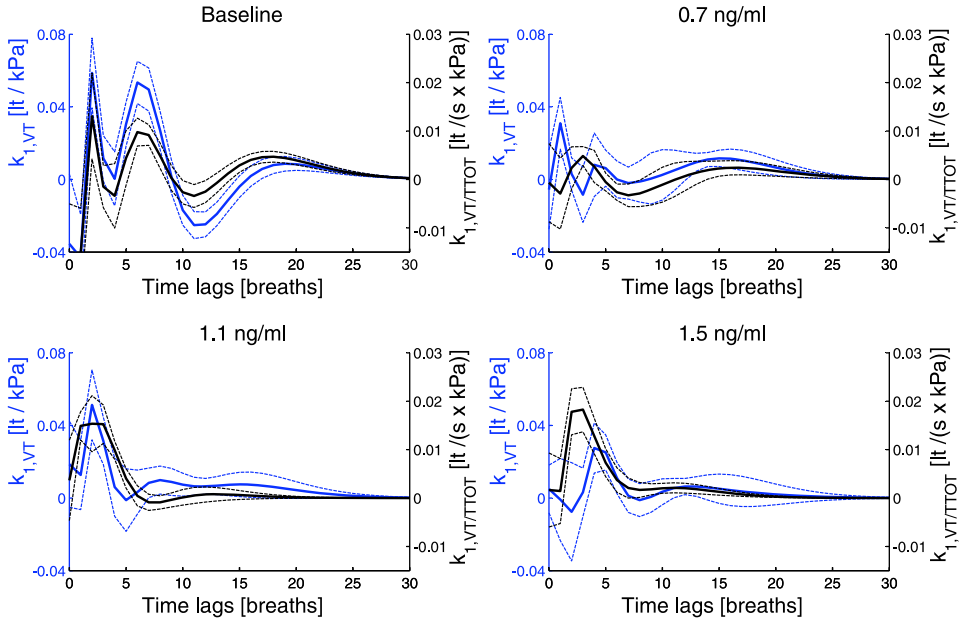

Fig. 4. Averaged impulse response (k_1 in *Eq. 1* for $Q = 1$) for the chemoreflex pathway, whereby both VT (blue) and VT/TTOT (black) were used to assess ventilatory variability. Both measures of ventilation yielded similar results, especially during baseline, where 2 main positive peaks are observed around 4 and 8 breaths (after accounting for the 2-breath pure time delay). Remifentanil decreased the impulse response values, particularly of the second peak. A secondary positive peak was also observed between 15 and 20 breaths (*top left* panel). Remifentanil infusions were 0.7, 1.1, and 1.5 ng/ml.

on the diagonal (i.e., $[f_1,f_1]$) of this plot quantify the quadratic effect of input oscillations at f_1, whereas off-diagonal values (i.e., $[f_1,f_2]$) quantify the contribution of nonlinear interactions between input oscillations at f_1 and f_2. In general, the second-order kernels exhibited peaks at locations similar to their first-order counterparts and were affected in a similar manner during remifentanil infusion. Therefore, the gain values of the chemoreflex second-order kernels reduced during remifentanil infusion and their power was shifted to lower frequencies (e.g., Fig. 6, *bottom right*). We note also that the second-order kernels were found to be more variable across subjects relative to their first-order counterparts. The spectral power of the frequency responses of Figs. 5–6 is shown in Fig. 7 for both model outputs (VT and VT/TTOT) in the case of linear and nonlinear models (Fig. 7, *A* and *B*, respectively). A decrease was generally observed in the spectral power of k_1 (linear models), as well as both k_1 and k_2 (nonlinear models). This decrease was statistically significant only during the lowest level of remifentanil infusion (0.7 ng/ml) for VT; however, more pronounced differences were observed when VT/TTOT was used as the model output.

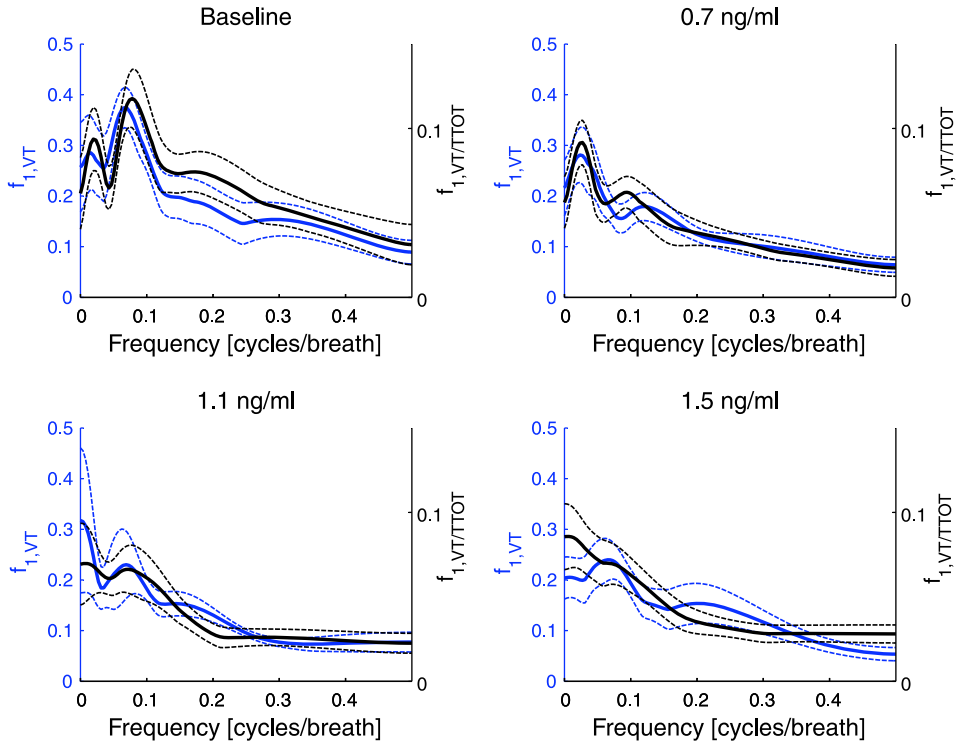

Fig. 5. The impulse responses of the chemoreflex pathway of Fig. 3 in the frequency domain when both VT (blue) and VT/TTOT (black) were used as measures of ventilatory variability. A resonant peak at 0.07 cycles/breath (i.e., corresponding to $P_{ET_{CO_2}}$ stimuli with periods of about 14 breaths) was observed during baseline, while most of the impulse response spectral power was shifted to lower frequencies during remifentanil infusion. Both measures of ventilation yielded similar results. Remifentanil infusions were 0.7, 1.1, and 1.5 ng/ml.

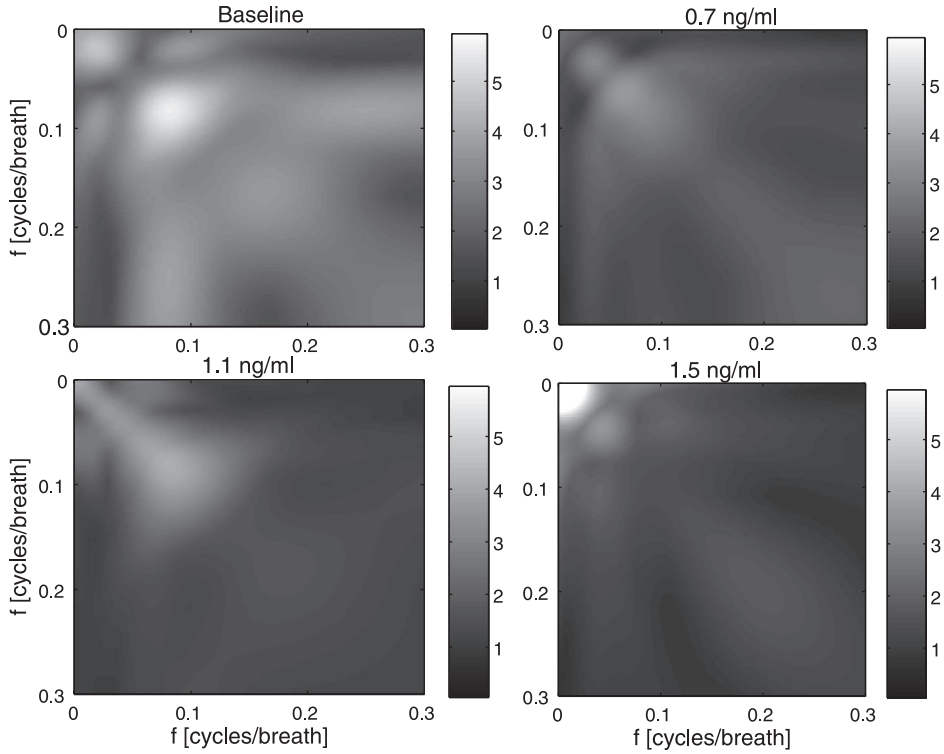

Fig. 6. Averaged 2nd-order kernels for the chemoreflex pathway in the 2-dimensional frequency domain when VT was used as a measure of ventilatory variability. The gain values of the 2nd-order kernels reduced during remifentanil infusion, and their power was shifted to lower frequencies in a manner similar to their 1st-order counterparts (see Fig. 5). Remifentanil infusions were 0.7, 1.1, and 1.5 ng/ml.

System dynamics: $V \rightarrow P_{ET_{CO_2}}$ pathway. The averaged impulse response for the reverse branch of the ventilatory loop ($V \rightarrow P_{ET_{CO_2}}$) is shown in Fig. 8 in the time domain when both VT (blue) and VT/TTOT (black) were considered as the model inputs. The form of the impulse responses suggests that an increase in tidal volume (or breath-to-breath ventilation) will lead to a decrease in $P_{ET_{CO_2}}$, with the maximum effects occurring almost instantaneously, i.e., within the first two breaths from the onset of the ventilatory change. It also suggests that the dynamic effects of these changes occur mainly within the first 5 breaths and cease before 20 breaths, since the impulse response values drop to zero before this point. Remifentanil infusion did not alter these characteristics; however, the impulse response values increased considerably at all infusion levels, suggesting a stronger dynamic effect of VT (or VT/TTOT) variability on $P_{ET_{CO_2}}$. This is reflected on the spectral power of the linear and nonlinear model components, calculated as above, which are shown in Fig. 9. Note that in this case k_1 exhibited a low-pass characteristic (not shown separately) due to its negative values at all time lags. The spectral power of k_1 increased significantly for both linear and nonlinear models, with the increase being more prominent in the latter case ($P < 0.01$ during all remifentanil levels for VT). The spectral power of the second-order model components k_2 increased as well ($P < 0.05$ at 0.7 ng/ml).

DISCUSSION

We have demonstrated that infusion of remifentanil leads to irregularity of the respiratory pattern during spontaneous respiration, with an associated increase in the mean and coefficient of variability of $P_{ET_{CO_2}}$. Moreover, it decreased the strength of the dynamic effect of natural $P_{ET_{CO_2}}$ variability on tidal volume and breath-to-breath ventilation, but increased the reverse relationship, i.e., the effect of ventilatory variability on $P_{ET_{CO_2}}$. Nonlinear, rather than linear, models best described these dynamic relationships. Collectively, these findings suggest the potential use of data-driven system modeling techniques to identify drug-induced changes on respiratory control on a systems level, employing experimental data from minimally invasive protocols.

Respiratory Variables

Remifentanil caused dose-dependent increases in the mean value of $P_{ET_{CO_2}}$, which also became more variable. The dose-dependent decrease in respiratory rate was associated with a profound prolongation of mean expiratory time (TE), but effects on inspiratory time were seen only at the highest dose.

Spectral power, which is calculated by integrating the PSD function of a signal, quantifies the variability of time-series data within different frequency ranges. The spectral analysis of the $P_{ET_{CO_2}}$ and VT time series confirmed that most of their power resides in the low-frequency range (below 0.3 cycles/breath), in agreement with previous studies (36). Therefore, we focused our analysis in this frequency range. The PSD of $P_{ET_{CO_2}}$, exhibited increased values over the entire range during remifentanil infusion (Fig. 2), whereas its VT counterpart increased above 0.02 cycles/breath, albeit less markedly. The corresponding spectral power values are in agreement with the rest of the physiological measurements in Table 1, i.e., both $P_{ET_{CO_2}}$ and VT became more variable during remifentanil infusion.

Dynamic Models

Whereas spectral analysis provides information about the relative magnitude of different oscillatory patterns that reside

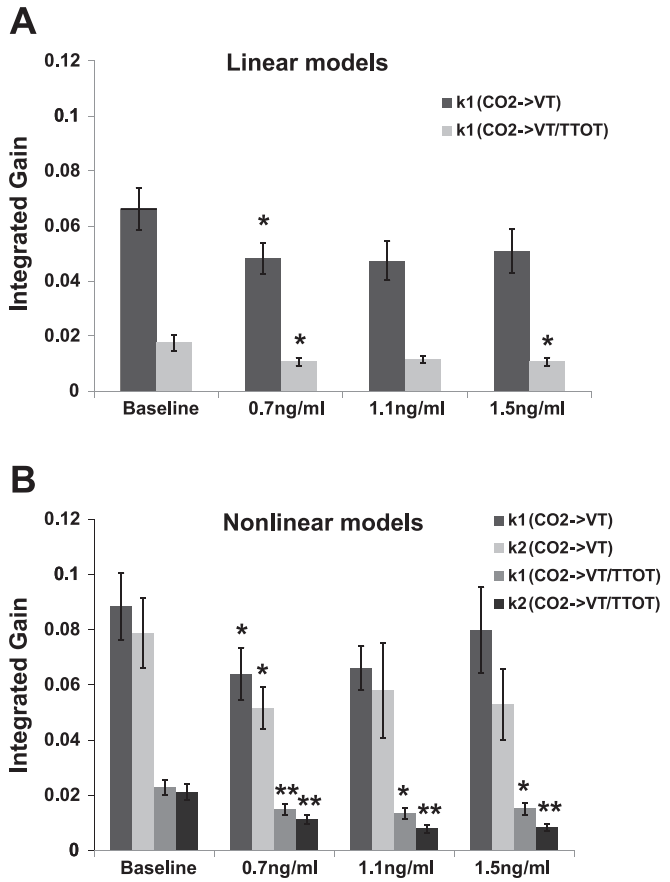

Fig. 7. Spectral power of the 1st- and 2nd-order Volterra kernels for linear (*A*) and nonlinear (*B*) models chemoreflex pathway. In the case of linear models, the impulse response (k_1) spectral power between 0 and 0.3 cycles/breath decreased during remifentanil infusion, while in the case of nonlinear models, the spectral power of both the linear and nonlinear components decreased during remifentanil infusion. The observed differences were more pronounced when V_T/T_{TOT} was used as a measure of ventilation (lower *P* values in all cases). Remifentanil infusions were 0.7, 1.1, and 1.5 ng/ml. $*P < 0.05$, $**P < 0.01$ compared with baseline.

in respiratory time series and how these are affected by remifentanil, it does not provide any information about whether these patterns are correlated or about the strength of these correlations at different frequency bands and at different remifentanil levels. However, the influence of the spontaneous variability of $P_{ET_{CO_2}}$ on fluctuations of breath-to-breath V_T variability has been demonstrated by application of a $P_{ET_{CO_2}}$ buffering technique, which reduced fluctuations in $P_{ET_{CO_2}}$ and V_T below 0.10 cycles/breath (29). Moreover, coherent oscillations between $P_{ET_{CO_2}}$ and mean inspiratory flow V_I/T_I in the frequency domain, in agreement with a closed-loop model of the chemoreflex feedback, have been also reported (36). To quantify these correlations, we have employed a nonlinear data-driven modeling approach that has been used extensively to model physiological systems (24). The results of our study extend the aforementioned observations to both pathways of the ventilatory loop (Fig. 1), examining for dynamic nonlinearities as well.

Spontaneous ventilatory variability arises from two components: V_{CO2}, which is the result of the causal effects of P_{CO_2} variations (chemical drive) and is captured by the employed dynamic models (Fig. 3*B* and Figs. 4–6), and V_d, which reflects the effects of all other exogenous physiological factors (including sighs) and is viewed as a disturbance term, i.e., it corresponds to the model residuals. Likewise, $P_{ET_{CO_2}}$ variability includes a ventilatory-related component $P_{ET_{CO_2},V}$ (captured by the corresponding dynamic models; Fig. 3*A* and Fig. 8) and a disturbance term $P_{ET_{CO_2},d}$, which corresponds to the residuals of the $V \rightarrow P_{ET_{CO_2}}$ models.

Model Performance

The output prediction NMSE (Table 2) was used as a measure of model performance. The relatively high NMSE values obtained for both pathways reflect the fact that the resting variability of $P_{ET_{CO_2}}$ and V_T (or V_T/T_{TOT}) is determined by multiple physiological factors, operating in a complex and closed-loop manner (8, 21). In the case of respiratory variability, significant influences that are part of the "disturbance" signal V_d (Fig. 1), which corresponds to the nonchemical respiratory drive, are exerted by inputs from cortical centers due to behavioral and volitional modulation, the tonic input of the reticular activating system during wakefulness, as well as changes in cardiovascular parameters (e.g., cardiac output and blood pressure or cerebral blood flow oscillations), due to the intricate coupling between the cardiovascular and respiratory systems. These influences may be stochastic (broadband) or periodic (21). As a result, similar ventilatory patterns may arise from different chemical and nonchemical components. Our results (nonlinear models; Table 1) suggest an increase in the chemical drive of ventilation during remifentanil infusion. Since the magnitude of the $P_{ET_{CO_2}} \rightarrow V$ model dynamics decreased (Figs. 4–7), this increase was due to the increased $P_{ET_{CO_2}}$ variability. Also, the fact that ventilatory variability, which comprises the net effect of the chemical and nonchemical components, increased less markedly (Fig. 2 and Table 1) implies a relative decrease in the nonchemical drive. Likewise, the $P_{ET_{CO_2}}$ disturbance signal is influenced by the aforementioned and other factors, such as metabolism, wakefulness, level of arousal, sleep state, and arterial P_{O_2} (Pa_{O_2}) level (8). We have successfully maintained these parameters as constant as possible, instructing subjects to remain awake and keeping $P_{ET_{O_2}}$ constant.

Nonlinear models reduced the NMSEs significantly, indicating the presence of dynamic nonlinearities between $P_{ET_{CO_2}}$ and V_T variations. The Laguerre expansion technique used in this study does not result in a dramatic increase in the number of free parameters in the case of nonlinear models, which is a problem often encountered in practice, especially for short data sets. In our case, the estimation of 22 free parameters [expansion coefficients, Laguerre parameter α, which determines the decay characteristics of the Laguerre basis (25), and constant term] was required, compared with 7 for linear models. Therefore, the large decrease in the nonlinear NMSE is unlikely to be due to the increase in model complexity alone, which is also taken into account in the determination of model structure. The validity of the nonlinear model terms is also corroborated by the fact that they exhibited similar trends to their linear counterparts (Figs. 7 and 9). The increased variability of the second-order kernels could be due to that they express interactions between different signal frequency components (i.e., they are characterized by more "degrees of freedom" in this context).

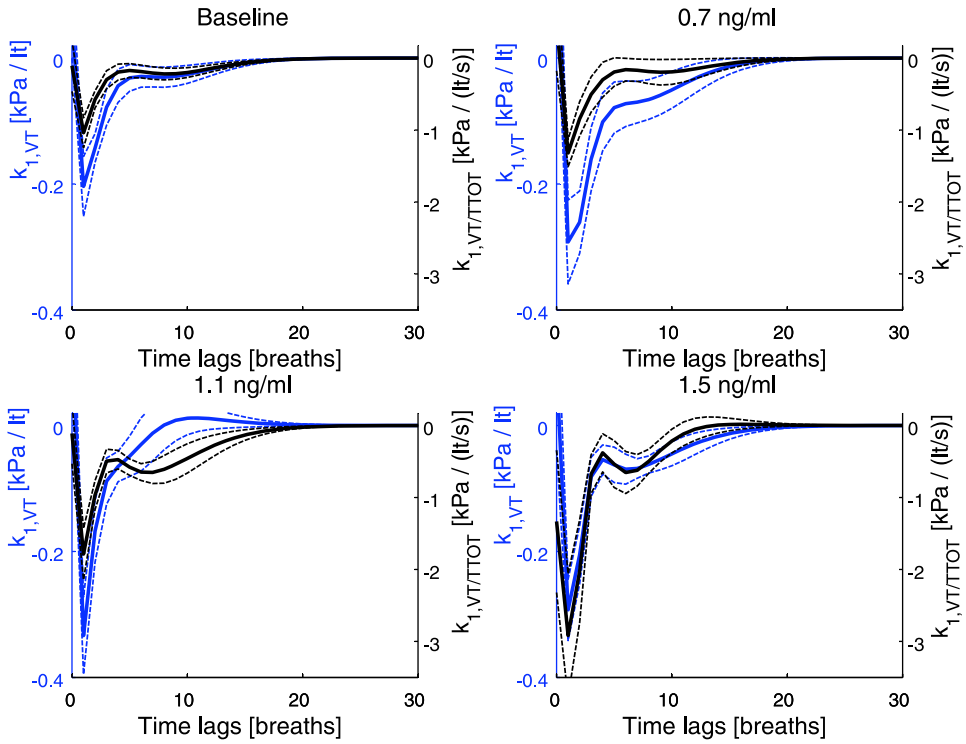

Fig. 8. Averaged impulse response (k_1 in *Eq. 1* for $Q = 1$) for the V $\rightarrow$ $P_{ET_{CO_2}}$ pathway when both VT (blue) and VT/TTOT (black) were used as measures of ventilatory variability. A main negative peak is observed at 1 breath, i.e., the dynamic effects of a VT (or VT/TTOT) change on $P_{ET_{CO_2}}$ are almost instantaneous. The impulse response drops to zero before 20 breaths in all cases. The waveform of the obtained impulse responses did not change during remifentanil; however, their values increased considerably during all infusion levels. Remifentanil infusions were 0.7, 1.1, and 1.5 ng/ml.

The presence of nonlinear (chaotic) dynamics in spontaneous respiratory volume variability has been reported by Wysocki et al. (38). On the other hand, the steady-state chemoreflex response, i.e., the relation between the mean values of $P_{ET_{CO_2}}$ and ventilation, has been shown to be relatively linear (9); however, note that in the present study we are examining the dynamic relation between spontaneous fluctuations around the mean values, whereby the latter may be viewed as the system "operating point." Regarding the reverse branch, it has been suggested that the influence of VT on CO_2 exhibits nonlinear characteristics in the case of large VT variations (6, 36); also, the gas exchange equations are characterized by nonlinear behavior. Our results suggest that the presence of nonlinearities is also significant in the interrelationships between VT (and VT/TTOT) and $P_{ET_{CO_2}}$ during resting conditions. The Laguerre expansion technique was used in a similar context by Asyali et al. (1), where the loop gain was obtained in normal subjects and patients with obstructive sleep apnea (OSA) during sleep by inducing transient arousals, with the OSA subjects exhibiting a tendency for higher average loop gains between 0.01 and 0.05 Hz, as well as more rapid and underdamped dynamics. However, in that study, the ventilatory impulse response was estimated as a whole, i.e., by using an autoregressive model to quantify the dependence of respiratory drive on its previous values. Here, we have obtained dynamic models of the two ventilatory branches separately.

System Dynamics: $P_{ET_{CO_2}} \rightarrow V$ Pathway

We removed deep breaths (sighs) from the VT and VT/TTOT time series before model estimation in the $P_{ET_{CO_2}} \rightarrow$ V pathway because sighs are not caused by $P_{ET_{CO_2}}$ changes, and their inclusion could have affected the model estimates. The same approach was employed by Van den Aardweg et al. (36). We also hypothesized a two-breath time delay in the effects of $P_{ET_{CO_2}}$, due to the lung-to-carotid body and lung-to-brain transport delays (20), in agreement with previous studies (20, 34, 36). Note that applying data-driven pure time-delay estimation methods (30) did not yield reasonable results in many cases, possibly due to the influence of the ventilatory disturbance term (nonchemical drive) and its propagation through the respiratory loop. Moreover, using delay values between one and four breaths did not affect the performance (i.e., NMSE value) of the employed models or the form of the kernel estimates to a large extent. Hence, we selected the use of a time delay of two breaths in all cases, although it is possible that the delay is reduced (e.g., to 1 breath) during the higher remifentanil levels, as the average TE increased significantly and, although we do not have a direct measure, cardiac output is likely to have decreased mildly.

The form of the impulse response between $P_{ET_{CO_2}}$ and VT (or VT/TTOT; Fig. 4), which is predominantly positive in all cases, agrees qualitatively with the previously well-described effects of $P_{ET_{CO_2}}$ on ventilation, i.e., an increase in $P_{ET_{CO_2}}$ results in an increase in VT (or VT/TTOT) some breaths later. Note also that the linear component obtained from linear and nonlinear models exhibited similar characteristics. The spectral peaks of the $P_{ET_{CO_2}} \rightarrow$ V dynamic models during baseline (Fig. 5, *top left*) generally agree with the results of Van den Aardweg et al. (36) , who reported coherent oscillations between $P_{ET_{CO_2}}$ and VI/TI below 0.15 cycles/breath with a peak observed around 0.08 cycles/breath for the averaged gain by utilizing coherence analysis, which is a measure of the strength of the linear relation between the two signals.

The multiphasic characteristic observed during baseline (Fig. 4, *top left*) possibly reflects the closed-loop nature of respiratory control, as an initial perturbation in $P_{ET_{CO_2}}$ will cause a change in tidal volume that has an opposite effect on $P_{ET_{CO_2}}$, and that these oscillations eventually get damped over

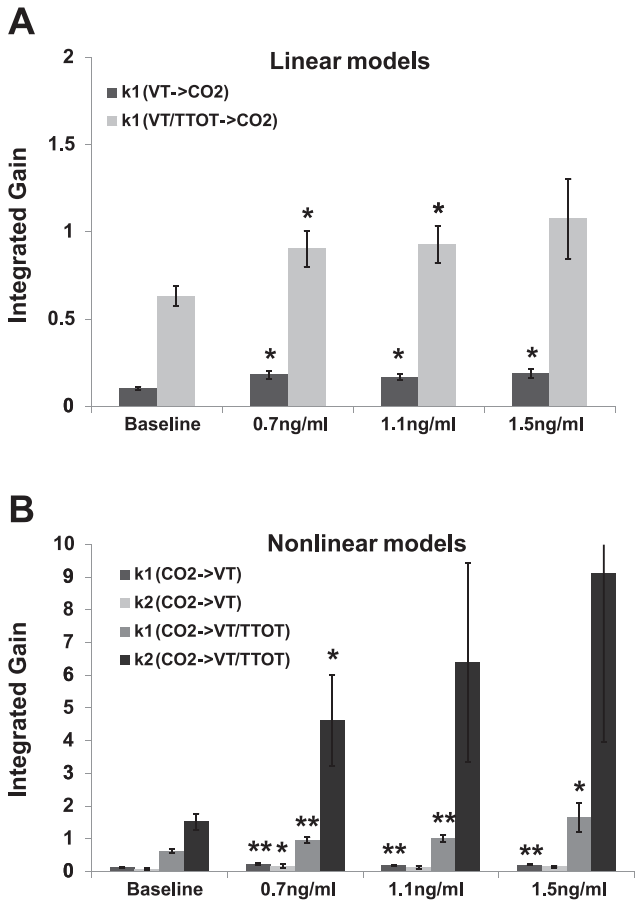

Fig. 9. Spectral power of the 1st- and 2nd-order Volterra kernels k_1 and k_2 for linear (*A*) and nonlinear (*B*) models, V $\rightarrow$ $P_{ET_{CO_2}}$ pathway. The spectral power of the 1st- and 2nd-order kernels increased significantly during remifentanil infusion (all levels). Remifentanil infusions were 0.7, 1.1, and 1.5 ng/ml. $^*P < 0.05$, $^{**}P < 0.01$ compared with baseline.

~30 breaths. The first two peaks of this response (at about 4 and 8 breaths, taking into account the 2-breath time delay hypothesized for the effects of $P_{ET_{CO_2}}$) may reflect the function of the fast peripheral carotid chemoreceptors. Interestingly, the relative location of these main peaks, as well as the secondary peak observed around 20 breaths, seems to correspond with the results of Pedersen et al. (34) regarding the time constants of the peripheral and central chemoreceptors; however, direct comparisons should be made with caution, as in that study a two-compartment differential equation model and a multifrequency binary $P_{ET_{CO_2}}$ sequence during hypoxic and hyperoxic conditions were used, resulting in a wide range of time constants.

We maintained a constant level of mild hyperoxia (~30 kPa); therefore, we expect that function of the peripheral chemoreflex was slightly depressed (34) and this effect should be constant throughout the study. On the other hand, hypoventilation and apneas may induce arterial hypoxemia, which has independent effects on the peripheral chemoreflex. Therefore, we used a manual dynamic end-tidal forcing technique (33, 37) to maintain Pa_{O_2} constant and avoid variability in peripheral chemoreceptor activation. Finally, opioids have a strong effect on the peripheral chemoreflex (2) and the contribution of a slightly elevated Pa_{O_2} is unlikely to influence the results significantly relative to this.

The spectral power of the $P_{ET_{CO_2}} \rightarrow$ V system dynamics decreased during remifentanil administration (Fig. 7), suggesting that arterial CO_2 has a less pronounced effect on the respiratory control centers (i.e., decreased chemosensitivity). We initially selected VT as a measure of ventilatory variability to differentiate motor output from effects on timing (predominantly TE). Using VT/TTOT as the system output yielded similar system dynamics to VT, especially during baseline, while the results were affected more during the highest remifentanil level, due to the irregularity induced on TE (and consequently TTOT). The differences in the integrated gain of the first- and second-order kernels were more pronounced for VT/TTOT, possibly suggesting that it is a more sensitive measure for assessing chemoresponsiveness during resting conditions. Note that we also examined other frequently used measures of ventilatory variability (9), i.e., mean inspiratory flow VT/TI and expiratory ventilation VT/TE, and the results were similar to VT and VT/TTOT, respectively. This is expected since TI was generally less variable and not affected substantially by remifentanil, whereas remifentanil-induced changes in TTOT were mainly caused by changes in TE.

Our findings of increased respiratory variability and increased TE generally agree with the three other human studies of opioid effects on breath timing during spontaneous respiration and confirm that remifentanil has similar respiratory effects to other opioids. Leino et al. (22) demonstrated increased variability of respiratory timing (but not VT) with morphine and oxycodone infusion. The findings of Bouillon et al. (4) were similar (although they noted increased variability of both VT and TE). Ferguson and Drummond (14) demonstrated, in a group of anesthetized humans, that fentanyl affects respiratory timing to a greater effect than VT. The subtle differences in the findings of studies are likely to represent differences in statistical approaches used. In none of these studies were detailed time-series analyses reported, as in the present study.

Mellen et al. (26) investigated the mechanism of respiratory depression in the pre-Bötzinger complex in neonatal rats. They found that irregular breathing was caused by intermittent interruption of communication between the pre-Bötzinger complex and the retrapezoid nucleus, leading to a "quantal" pattern of respiratory depression. It is difficult, however, to relate these findings to conscious adult humans, where so many other factors determine respiratory output. If remifentanil were to interrupt motor output independently of the tonic effect of CO_2 as in the study of Mellen et al. (26), then this may partially explain respiratory depression, beyond reduced chemosensitivity. We did not observe quantal slowing and are therefore unable to dissociate these two effects in the present study.

Intrabreath oscillations in Pa_{CO_2} may have a strong effect on respiration (7), independent of mean Pa_{CO_2} value, and this effect is stronger in chronic hypoxia of high altitude, where the ventilatory sensitivity to CO_2 is increased. We could therefore speculate that the increased $P_{ET_{CO_2}}$ variability seen in the present study may help maintain ventilation during opioid-induced respiratory depression; therefore it would be interesting to examine the effects of a CO_2 buffering technique to reduce this variability.

On the other hand, sleep, which is accompanied by an increase in steady-state arterial CO_2, has been shown to decrease the ventilatory responses to hypercapnia and hypoxia (16, 19). In the present study, we have observed this latter

effect: despite remifentanil increasing mean $P_{ET_{CO_2}}$ and its variability around the mean, there is reduced ventilatory sensitivity.

System Dynamics: $V \rightarrow P_{ET_{CO_2}}$ Pathway

The $V \rightarrow P_{ET_{CO_2}}$ impulse responses (Fig. 8) quantify the dynamics of the reverse pathway of the ventilatory loop. Their waveforms, which are negative over all time lags, correspond to the well-known effects of respiratory changes, i.e., an abrupt increase in VT (or VT/TTOT) results in a rapid decrease in $P_{ET_{CO_2}}$. Its time extent suggests that this change settles back within the subsequent 20 breaths. Remifentanil infusion did not have a profound effect on the timing of the $V \rightarrow P_{ET_{CO_2}}$ impulse responses; however, it increased its values to a similar extent at all remifentanil levels for both measures of ventilatory variability considered, suggesting an increased $P_{ET_{CO_2}}$ sensitivity to ventilatory changes. Hypercapnia may contribute to this increased sensitivity, due to greater CO_2 excretion per breath as a simple mass effect, as similar observations have been reported during sleep, which also induces hypercapnia (19). Other possible factors could include decreased cardiac output and/or metabolic rate. However, we consider this as being unlikely, as the levels of remifentanil examined in the present study are relatively low.

Ventilatory Stability

The stability of the ventilatory control loop is determined by the loop gain, i.e., the product of the controller and plant gains (21) in the case of linear models (it is not straightforward to compute it in the case of nonlinear models). When VT was used as a measure of ventilatory variability, the integrated loop gain between 0 and 0.3 cycles/breath was 0.026 ± 0.003 at baseline and 0.030 ± 0.005 at 1.5 ng/ml, (P = not significant), as the decrease in the controller ($P_{ET_{CO_2}} \rightarrow$ VT) gains induced by remifentanil was counterbalanced by a more pronounced increase in the plant (VT $\rightarrow P_{ET_{CO_2}}$) gains. The values of integrated loop gain values did not change significantly also when VT/TTOT was used (0.041 ± 0.007 during baseline, 0.036 ± 0.004 at 1.5 ng/ml of remifentanil infusion, P = not significant). In this case, the decrease in the controller gain and the increase in the plant gain were both less pronounced. These results should be interpreted with some caution, as the obtained system dynamics are "closed-loop" estimates and may be therefore affected by correlations between the input/output and disturbance terms (see also *Limitations*). Further changes in loop gain may arise from altered delays in the ventilatory loop; however, we consider this unlikely, as these would require large changes in cardiac output, for which we had no direct evidence.

Limitations

The changes observed in resting ventilation are dependent on the interaction of drug and CO_2 kinetics (3). In the present study we investigated the response to a steady-state infusion of remifentanil. This drug is convenient to study because it has a short context-insensitive half-life, and plasma (and effect site) concentrations can easily be manipulated. However, it is not commonly used as an analgesic except in anesthetic practice, as small errors in infusion rate can lead to severe respiratory depression. As it is so potent, the same dose of remifentanil can cause varying respiratory effects that are dependent on its rate of delivery and are fully explained in a modeling study by Bouillon et al. (3). In the present study we used relatively low doses of remifentanil and waited for stabilization of effect site concentrations before making measurements. Although we believe that the dose range that we employed is likely to be applicable to clinical analgesia, further studies investigating more commonly used drugs (e.g., morphine) are required. It would be especially interesting to use this methodology to investigate effects of opioids with effects on other receptor-mediated systems [e.g., tramadol (22)] or partial agonists [e.g., buprenorphine (12)] that have been shown to have different effects on respiration than pure μ-opioid agonists such as remifentanil.

Unlike studies that examine respiration at predetermined CO_2 and oxygen levels that open the ventilatory feedback loop, our experimental approach does not allow the same precision of measuring the hypoxic and hypercapnic ventilatory responses. Since it is based on using smaller natural fluctuations around the mean, the sensitivity it yields may be further increased; for instance, the decrease observed in the chemoreflex pathway kernels (Figs. 4–7) was not gradual for higher remifentanil levels. In this context, improvement could be achieved by investigating the optimal recording duration and/or the effect of alternative input patterns that would increase the chemical drive. These could include mild perturbations such as small CO_2 boluses (pseudorandom binary pulses) or occasional vital capacity breaths to cause brief hypocapnia. However, since the main advantage of our methodology is that it is more directly applicable to the clinical situation, as it allows examination of the system under natural, closed-loop operating conditions and does not require external experimental interventions, alternative stimuli would have to be carefully designed so that they do not perturb the system away from its natural state. We defer this to future studies.

Another consequence of the fact that the respiratory control system is probed under normal breathing, i.e., under natural, closed-loop conditions, is that the obtained model estimates are closed-loop responses. Therefore, they are possibly affected by the fact that the input, output, and disturbance signals are correlated and by the propagation of the latter around the loop, which are characteristics that are inherent in all closed-loop systems. To account for this, we removed a major fraction of the ventilatory disturbance signal (V_d)—deep breaths, which are clearly not caused by $P_{ET_{CO_2}}$ changes—before model estimation in the $P_{ET_{CO_2}} \rightarrow$ V pathway. The aforementioned effects are expected to be more pronounced in this pathway, as the dynamic effects of $P_{ET_{CO_2}}$ on VT (or VT/TTOT) are weaker than vice versa (see, e.g., Fig. 3). The design of alternative stimuli patterns could also help in further discriminating the "plant" from the "controller" responses, at the cost however of perturbing the control loop from its state of natural operation.

In conclusion, we have characterized the effects of low-dose remifentanil infusion on spontaneous respiration in detail by utilizing linear and nonlinear dynamic models, which suggests the potential use of data-driven system modeling techniques to identify drug-induced changes on respiratory control. This approach is particularly useful for investigating drug action in the clinical situation because it can derive useful information from a clinically relevant experimental paradigm.

ACKNOWLEDGMENTS

We thank Prof. Peter A. Robbins of Oxford University for helpful suggestions in improving the manuscript.

GRANTS

This study was supported by project grants from the Association of Anaesthetists of Great Britain and Ireland, and from the International Anesthesia Research Society. G. D. Mitsis is supported by the European Social Fund (75%) and National Resources (25%), Operational Program Competitiveness, General Secretariat for Research and Development (Program ENTER 04). K. T. S. Pattinson is supported by the Medical Research Council (UK).

REFERENCES

1. **Asyali MH, Berry RB, Khoo MCK.** Assessment of closed-loop ventilatory stability in obstructive sleep apnea. *IEEE Trans Biomed Eng* 49: 206–216, 2002.
2. **Bailey PL, Lu JK, Pace NL, Orr JA, White JL, Hamber EA, Slawson MH, Crouch DJ, Rollins DE.** Effects of intrathecal morphine on the ventilatory response to hypoxia. *N Engl J Med* 343: 1228–1234, 2000.
3. **Bouillon T, Bruhn J, Radu-Radulescu L, Andresen C, Cohane C, Shafer SL.** A model of the ventilatory depressant potency of remifentanil in the non-steady state. *Anesthesiology* 99: 779–787, 2003.
4. **Bouillon T, Bruhn J, Roepcke H, Hoeft A.** Opioid-induced respiratory depression is associated with increased tidal volume variability. *Eur J Anaesthesiol* 20: 127–133, 2003.
5. **BuSha BF, Stella MH.** State and chemical drive modulate respiratory variability. *J Appl Physiol* 93: 685–696, 2002.
6. **Chilton A, Stacy R.** A mathematical analysis of carbon dioxide respiration in man. *Bull Math Biol* 14: 1–18, 1952.
7. **Collier DJ, Nickol AH, Milledge JS, van Ruiten HJ, Collier CJ, Swenson ER, Datta A, Wolff CB.** Alveolar P_{CO_2} oscillations and ventilation at sea level and at high altitude. *J Appl Physiol* 104: 404–415, 2008.
8. **Crosby A, Robbins PA.** Variability in end-tidal P_{CO_2} and blood gas values in humans. *Exp Physiol* 88: 2003.
9. **Cunningham DJC, Robbins PA, Wolff CB.** Integration of respiratory responses to changes in alveolar partial pressures of CO_2 and O_2 and in arterial pH. In: *Handbook of Physiology. The Respiratory System.* Bethesda, MD: Am. Physiol. Soc., 1986, p. 475–528.
10. **Dahan A, Teppema LJ.** Influence of anaesthesia and analgesia on the control of breathing. *Br J Anaesth* 91: 40–49, 2003.
11. **Dahan A, Yassen A, Bijl H, Romberg R, Sarton E, Teppema L, Olofsen E, Danhof M.** Comparison of the respiratory effects of intravenous buprenorphine and fentanyl in humans and rats. *Br J Anaesth* 94: 825–834, 2005.
12. **Dahan A, Yassen A, Romberg R, Sarton E, Teppema L, Olofsen E, Danhof M.** Buprenorphine induces ceiling in respiratory depression but not in analgesia. *Br J Anaesth* 96: 627–632, 2006.
13. **Feldman JL, Del Negro CA.** Looking for inspiration: new perspectives on respiratory rhythm. *Nat Rev Neurosci* 7: 232–242, 2006.
14. **Ferguson LM, Drummond GB.** Acute effects of fentanyl on breathing pattern in anaesthetized subjects. *Br J Anaesth* 96: 384–390, 2006.
15. **Fiamma MN, Straus C, Thibault S, Wysocki M, Baconnier P, Similowski T.** Effects of hypercapnia and hypocapnia on ventilatory variability and the chaotic dynamics of ventilatory flow in humans. *Am J Physiol Regul Integr Comp Physiol* 292: R1985–R1993, 2007.
16. **Gothe B, Altose MD, Goldman MD, Cherniack NS.** Effect of quiet sleep on resting and CO_2-stimulated breathing in humans. *J Appl Physiol* 50: 724–730, 1981.
17. **Gray JM, Kenny GN.** Development of the technology for "Diprifusor" TCI systems. *Anaesthesia* 53*, Suppl* 1: 22–27, 1998.
18. **Khoo M, Marmarelis V.** Estimation of peripheral chemoreflex gain from spontaneous sigh responses. *Ann Biomed Eng* 17: 557–570, 1989.
19. **Khoo MC, Gottschalk A, Pack AI.** Sleep-induced periodic breathing and apnea: a theoretical study. *J Appl Physiol* 70: 2014–2024, 1991.
20. **Khoo MC, Kronauer RE, Strohl KP, Slutsky AS.** Factors inducing periodic breathing in humans: a general model. *J Appl Physiol* 53: 644–659, 1982.
21. **Khoo MCK.** Determinants of ventilatory instability and variability. *Respir Physiol* 122: 167–182, 2000.
22. **Leino K, Mildh L, Lertola K, Seppala T, Kirvela O.** Time course of changes in breathing pattern in morphine- and oxycodone-induced respiratory depression [see Comment]. *Anaesthesia* 54: 835–840, 1999.
23. **Mapleson WW.** The elimination of rebreathing in various semi-closed anaesthetic systems. *Br J Anaesth* 26: 323–332, 1954.
24. **Marmarelis V.** *Nonlinear Dynamic Modeling of Physiological Systems*. Piscataway, NJ: IEEE-Wiley, 2004.
25. **Marmarelis VZ.** Identification of nonlinear biological systems using Laguerre expansions of kernels. *Ann Biomed Eng* 21: 573–589, 1993.
26. **Mellen NM, Janczewski WA, Bocchiaro CM, Feldman JL.** Opioid-induced quantal slowing reveals dual networks for respiratory rhythm generation. *Neuron* 37: 821–826, 2003.
27. **Minto CF, Schnider TW, Egan TD, Youngs E, Lemmens HJ, Gambus PL, Billard V, Hoke JF, Moore KH, Hermann DJ, Muir KT, Mandema JW, Shafer SL.** Influence of age and gender on the pharmacokinetics and pharmacodynamics of remifentanil. I. Model development. *Anesthesiology* 86: 10–23, 1997.
28. **Minto CF, Schnider TW, Shafer SL.** Pharmacokinetics and pharmacodynamics of remifentanil. II. Model application. *Anesthesiology* 86: 24–33, 1997.
29. **Modarreszadeh M, Bruce EN.** Ventilatory variability induced by spontaneous variations of Pa_{CO_2} in humans. *J Appl Physiol* 76: 2765–2775, 1994.
30. **Muller T, Lauk M, Reinhard M, Hetzel A, Lucking CH, Timmer J.** Estimation of delay times in biological systems. *Ann Biomed Eng* 31: 1423–1439, 2003.
31. **Nieuwenhuijs D, Bruce J, Drummond GB, Warren PM, Dahan A.** Influence of oral tramadol on the dynamic ventilatory response to carbon dioxide in healthy volunteers. *Br J Anaesth* 87: 860–865, 2001.
32. **Pattinson KT.** Opioids and the control of respiration. *Br J Anaesth* 100: 747–758, 2008.
33. **Pattinson KT, Rogers R, Mayhew SD, Tracey I, Wise RG.** Pharmacological FMRI: measuring opioid effects on the BOLD response to hypercapnia. *J Cereb Blood Flow Metab* 27: 414–423, 2007.
34. **Pedersen ME, Fatemian M, Robbins PA.** Identification of fast and slow ventilatory responses to carbon dioxide under hypoxic and hyperoxic conditions in humans. *J Physiol* 521: 273–287, 1999.
35. **Sjoberg J.** *Non-linear System Identification With Neural Networks*. Linkoping, Sweden: Linkoping Univ., 1995.
36. **Van den Aardweg JG, Karemaker JM.** Influence of chemoreflexes on respiratory variability in healthy subjects. *Am J Respir Crit Care Med* 165: 1041–1047, 2002.
37. **Wise RG, Pattinson KTS, Bulte DP, Chiarelli PA, Mayhew SD, Balanos G, O'Connor D, Pragnell T, Robbins PA, Tracey I, Jezzard P.** Dynamic forcing of end-tidal carbon dioxide and oxygen applied to functional magnetic resonance imaging. *J Cereb Blood Flow Metab* 27: 1521–1532, 2007.
38. **Wysocki M, Fiamma MN, Straus C, Poon CS, Similowski T.** Chaotic dynamics of resting ventilatory flow in humans assessed through noise titration. *Respir Physiol Neurobiol* 153: 54–65, 2006.